

REPORT DOCUMENTATION PAGE				Form Approved OMB No. 0704-0188	
<p>Public reporting burden for this collection of information is estimated to average 1 hour per response, including the time for reviewing instructions, searching existing data sources, gathering and maintaining the data needed, and completing and reviewing this collection of information. Send comments regarding this burden estimate or any other aspect of this collection of information, including suggestions for reducing this burden to Department of Defense, Washington Headquarters Services, Directorate for Information Operations and Reports (0704-0188), 1215 Jefferson Davis Highway, Suite 1204, Arlington, VA 22202-4302. Respondents should be aware that notwithstanding any other provision of law, no person shall be subject to any penalty for failing to comply with a collection of information if it does not display a currently valid OMB control number. PLEASE DO NOT RETURN YOUR FORM TO THE ABOVE ADDRESS.</p>					
1. REPORT DATE (DD-MM-YYYY) June 2015		2. REPORT TYPE Briefing Charts		3. DATES COVERED (From - To) June 2015-June 2015	
4. TITLE AND SUBTITLE AB INITIO QUANTUM CHEMICAL REACTION KINETICS: RECENT APPLICATIONS IN COMBUSTION CHEMISTRY (Briefing Charts)				5a. CONTRACT NUMBER In-House	
				5b. GRANT NUMBER	
				5c. PROGRAM ELEMENT NUMBER	
6. AUTHOR(S) Ghanshyam L. Vaghjiani				5d. PROJECT NUMBER	
				5e. TASK NUMBER	
				5f. WORK UNIT NUMBER Q0RA	
7. PERFORMING ORGANIZATION NAME(S) AND ADDRESS(ES) Air Force Research Laboratory (AFMC) AFRL/RQRP 10 E. Saturn Blvd. Edwards AFB, CA93524-7680				8. PERFORMING ORGANIZATION REPORT NO.	
9. SPONSORING / MONITORING AGENCY NAME(S) AND ADDRESS(ES) Air Force Research Laboratory (AFMC) AFRL/RQR 5 Pollux Drive Edwards AFB CA 93524-7048				10. SPONSOR/MONITOR'S ACRONYM(S)	
				11. SPONSOR/MONITOR'S REPORT NUMBER(S) AFRL-RQ-ED-VG-2015-259	
12. DISTRIBUTION / AVAILABILITY STATEMENT Distribution A: Approved for Public Release; Distribution Unlimited.					
13. SUPPLEMENTARY NOTES Briefing Charts presented at 9th Int. Conf. Chemical Kinetics; Ghent, Belgium; 28 Jun 2015. PA#15351.					
14. ABSTRACT Briefing Charts					
15. SUBJECT TERMS					
16. SECURITY CLASSIFICATION OF:			17. LIMITATION OF ABSTRACT SAR	18. NUMBER OF PAGES 20	19a. NAME OF RESPONSIBLE PERSON Stefan Schneider
a. REPORT Unclassified	b. ABSTRACT Unclassified	c. THIS PAGE Unclassified			19b. TELEPHONE NO (include area code) 661-275-5759



***Ab initio* Quantum Chemical Reaction Kinetics: Recent Applications in Combustion Chemistry**

Ghanshyam L. Vaghjiani*

**9th ICCK
June 28, 2015**

***Propellants Branch
Rocket Propulsion Division
Aerospace Systems Directorate
Air Force Research Laboratory
AFRL/RQRP
10 E Saturn Blvd
Edwards AFB, CA 93524***

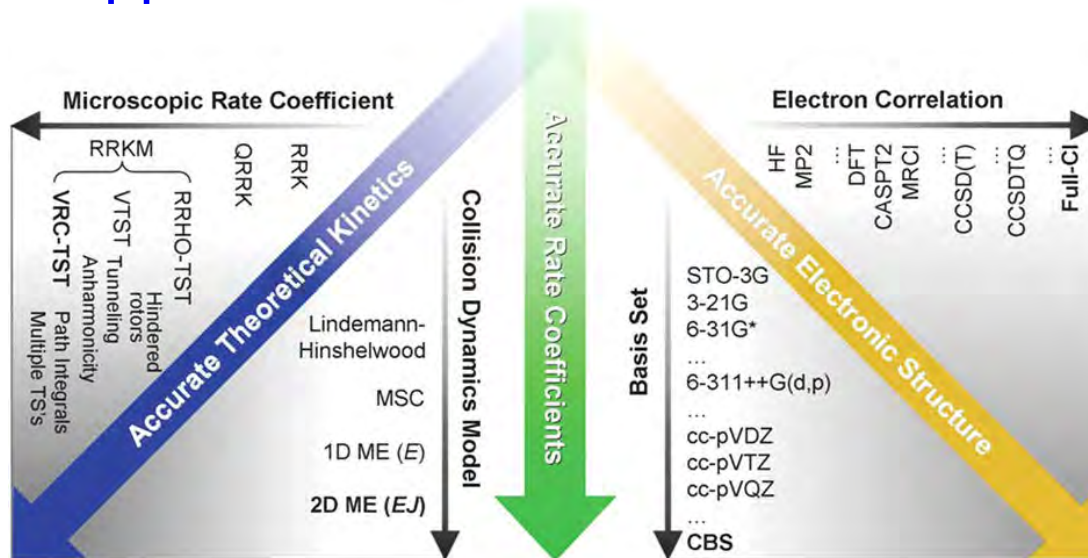
****Email: ghanshyam.vaghjiani@us.af.mil***



Why Quantum Chemical Reaction Kinetics Studies?



- Only Option When Experiments are not Possible or Limited
 - Combustion Conditions of P & T too Extreme to Probe
- Accuracy (E_a) can be as Good or Better Than Experiments
 - Thermochemical Accuracy Possible
 - Ideal for Branching Ratio Predictions for Closely Competing Reactions
- Can be a Cost Effective Alternate to Experiments
 - Hardware & Software Efficiencies Improving Constantly
- A Balanced Approach to Kinetics Calculations Recommended

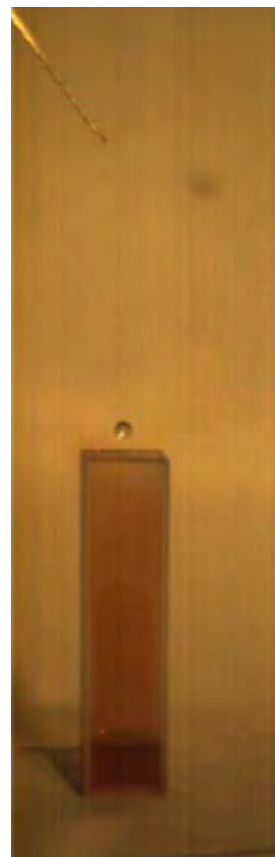




Our Interest in Combustion Chemistry



- Autoignition Chemistry
 - Low Temperature/Low Pressure Conditions
 - Bi-propellants



- Decomposition Chemistry
 - Emerging Energetic Materials
 - Explosives
 - Ionic Liquid Propellants



$\text{N}_2\text{H}_3 + \text{NO}_2$ Reaction Kinetics Perspective



- Radical Chemistry Modelling

- $\text{N}_2\text{H}_4/\text{NO}_2$ Autoignition

- Recent Works

- Only Theoretical Studies

- See Raghunath *et al.*, Adv. Quantum Chem., **69**, 253 (2014)..... $k_{298\text{ K}, 1\text{ atm}} = (2.3 \times 10^{-11})$
- See Daimon *et al.*, Sci. Tech. Energetic Materials, **74**, 17 (2013)..... $k_{298\text{ K}, 1\text{ atm}} = (1.6 \times 10^{-14})$?
- See Daimon *et al.*, J. Propul. Power, **30**, 707 (2014)..... $k_{298\text{ K}, 1\text{ atm}} = (1.9 \times 10^{-11})$
- Also, See Kanno *et al.*, DOI: 10.1021/acs.jpca.5b00987 (2015)



- This work

- Pulsed Laser Photolysis - Flow Tube MS Experiments

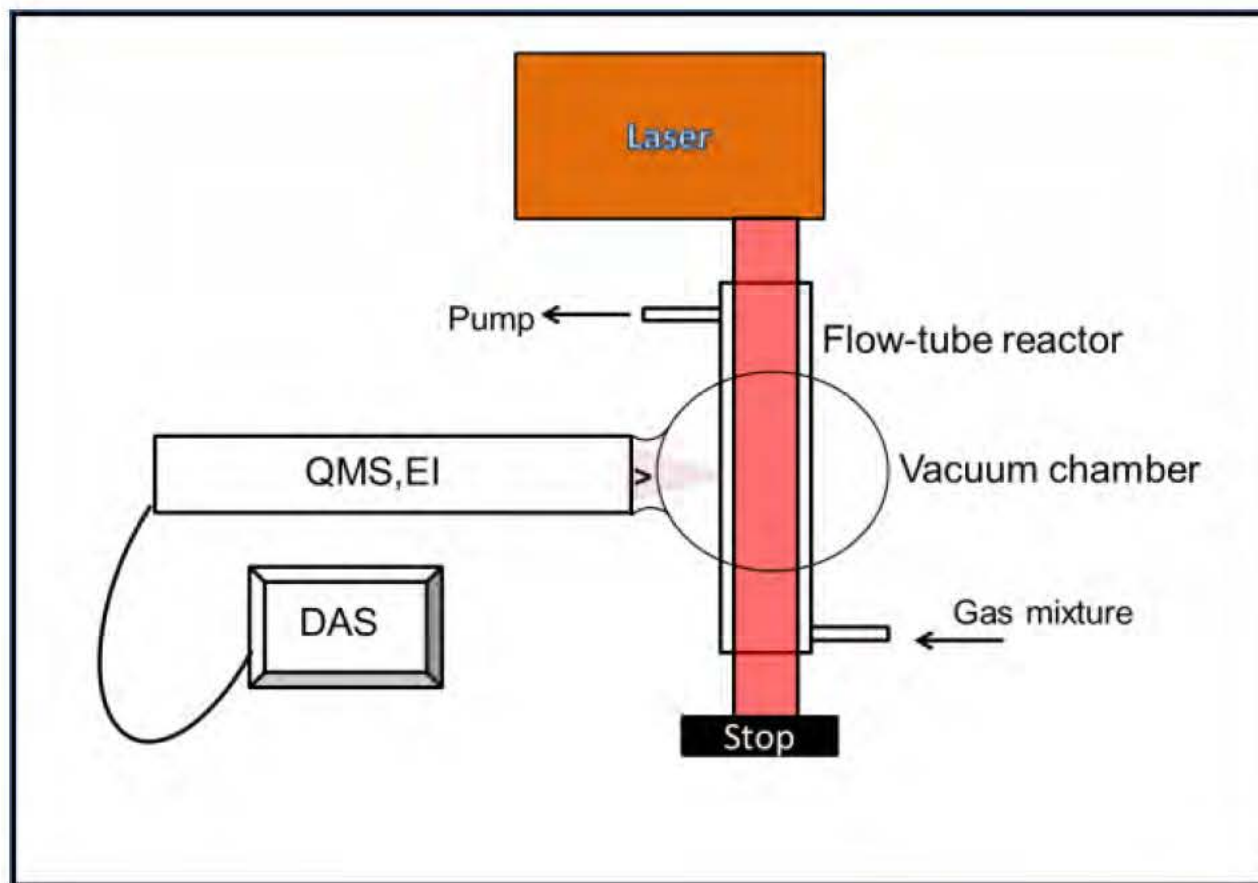
- First Experimental Determination

- Ab initio* Chemical Kinetics

- Multi-reference Second-order Perturbation and Coupled-cluster Methods: PES (Potential Energy Surface)
- RRKM (Rice–Ramsperger–Kassel–Marcus) Theory and Master Equation Simulations: k



Pulsed Laser Photolysis Flow Tube Apparatus





N_2H_3 Source & Flow Tube Chemistry



$\text{N}_2\text{H}_4 + h\nu \rightarrow \text{N}_2\text{H}_3 + \text{H}$	$\sigma_{193\text{ nm}} = 450 \times 10^{-20} \text{ cm}^2 \text{ molec}^{-1}$	1
$\text{NO}_2 + \text{H} \rightarrow \text{NO} + \text{OH}$	$k_2 = 1.3 \times 10^{-10} \text{ cm}^3 \text{ molecule}^{-1} \text{ s}^{-1}$	2
$\text{N}_2\text{H}_4 + \text{H} \rightarrow \text{N}_2\text{H}_3 + \text{H}_2$	$k_3 = 1.4 \times 10^{-13} \text{ cm}^3 \text{ molecule}^{-1} \text{ s}^{-1}$	3
$\text{N}_2\text{H}_4 + \text{OH} \rightarrow \text{N}_2\text{H}_3 + \text{H}_2\text{O}$	$k_4 = 3.6 \times 10^{-11} \text{ cm}^3 \text{ molecule}^{-1} \text{ s}^{-1}$	4
$\text{N}_2\text{H}_3 + \text{NO}_2 \rightarrow \text{N}_2\text{H}_2 + \text{HONO}$	k_5	5
$\text{N}_2\text{H}_3 + \text{NO}_2 \rightarrow \text{other products}$	k_6	6
$\text{HONO} \rightarrow \text{loss}$	$k_7 = 1 \text{ s}^{-1}$	7
$\text{N}_2\text{H}_3 \rightarrow \text{loss}$	$k_8 = 10 \text{ s}^{-1}$	8
$\text{H} \rightarrow \text{loss}$	$k_9 = 10 \text{ s}^{-1}$	9
$\text{OH} \rightarrow \text{loss}$	$k_{10} = 10 \text{ s}^{-1}$	10

$$[\text{HONO}] = (k_5[\text{NO}_2][\text{N}_2\text{H}_3]_0)(e^{-k_7 t} - e^{-k' t})/(k' - k_7)$$

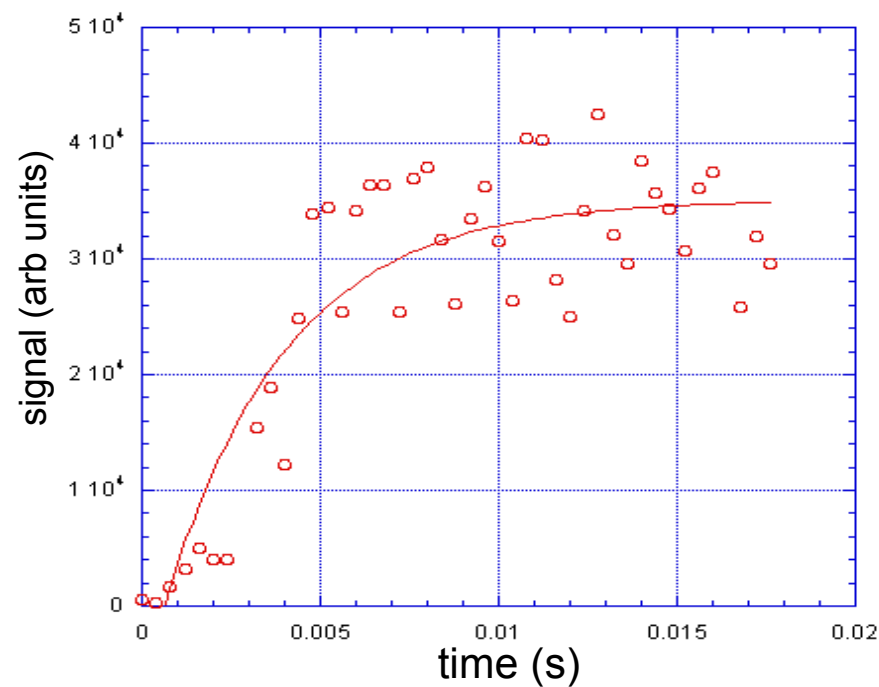
$$k' = (k_5 + k_6)[\text{NO}_2] + k_8$$

$$[\text{N}_2\text{H}_4] = 5 \times 10^{14}, [\text{H}] = 5 \times 10^{12}, [\text{NO}_2] = 1 \times 10^{13} \text{ to } 5 \times 10^{13} \text{ molecule cm}^{-3}$$

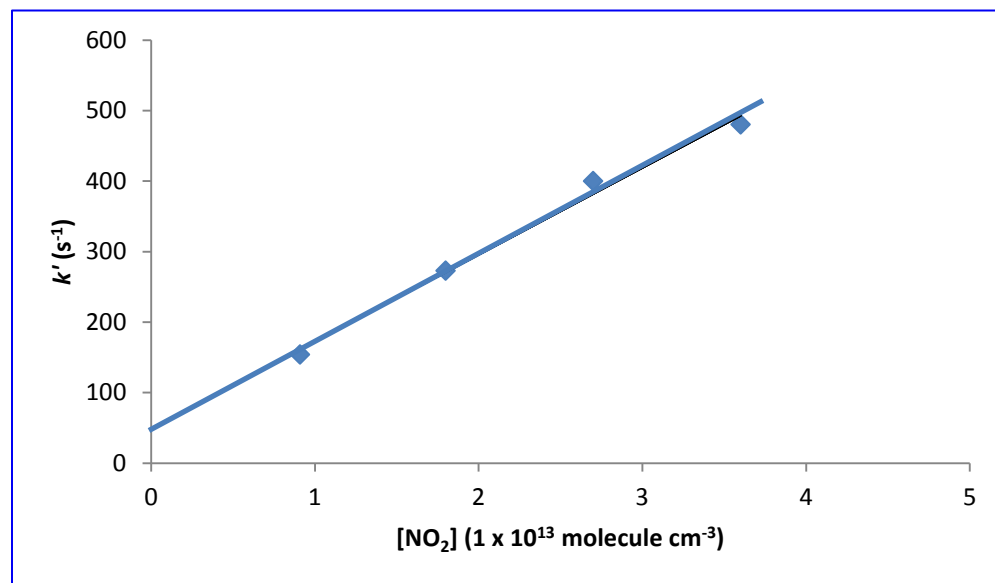


$\text{N}_2\text{H}_3 + \text{NO}_2$ Reaction Kinetics

Typical [HONO] Temporal Profile



Second-order Plot



$$k_{298 \text{ K}, 2 \text{ Torr N}_2} = (1.23 \pm 0.25) \times 10^{-11} \text{ cm}^3 \text{ molecule}^{-1} \text{ s}^{-1}$$



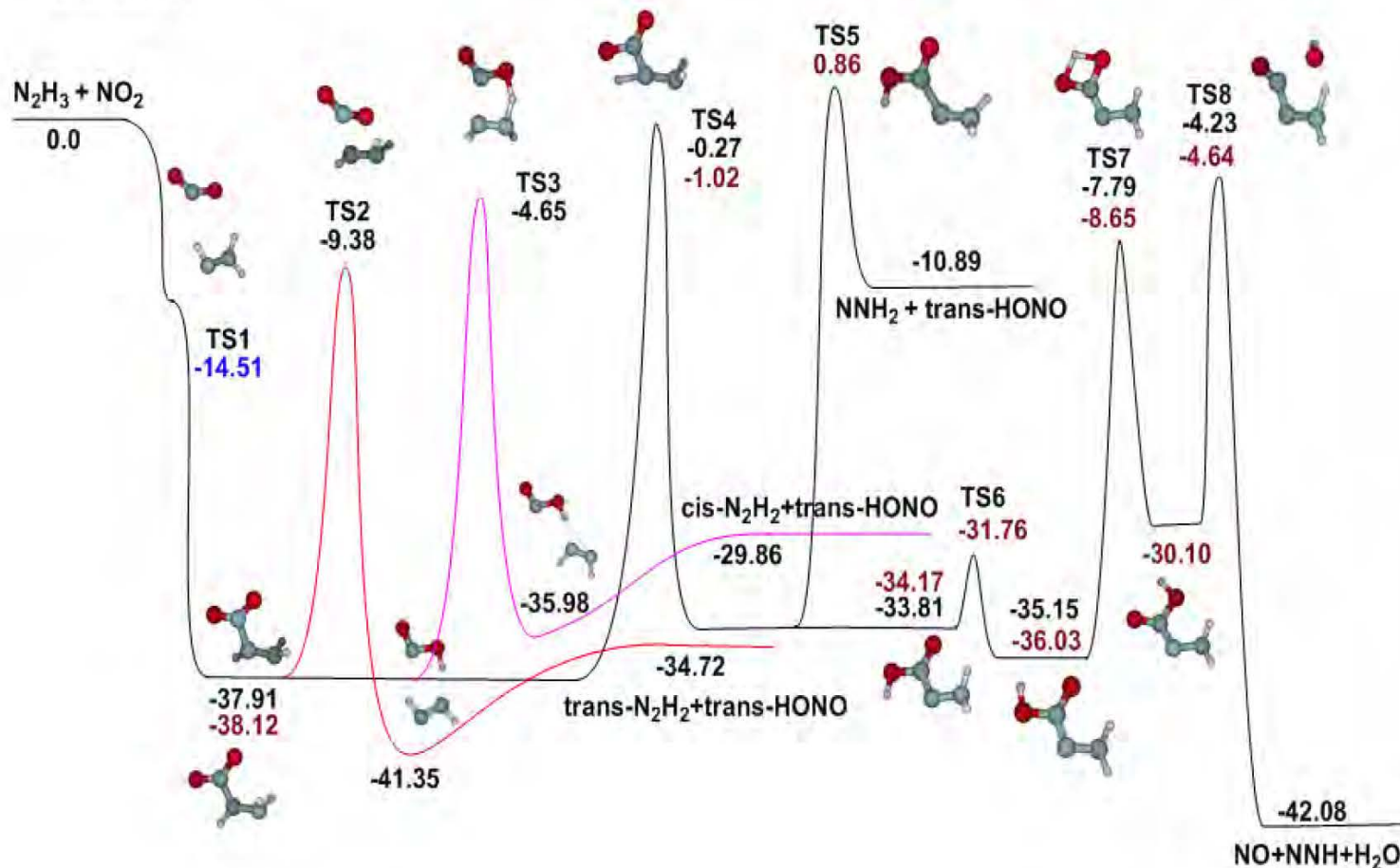
Potential Energy Surface for $\text{N}_2\text{H}_3\text{NO}_2$ Adduct Formation

CASPT2/CBS

RCCSD(T)/CBS//CASPT2

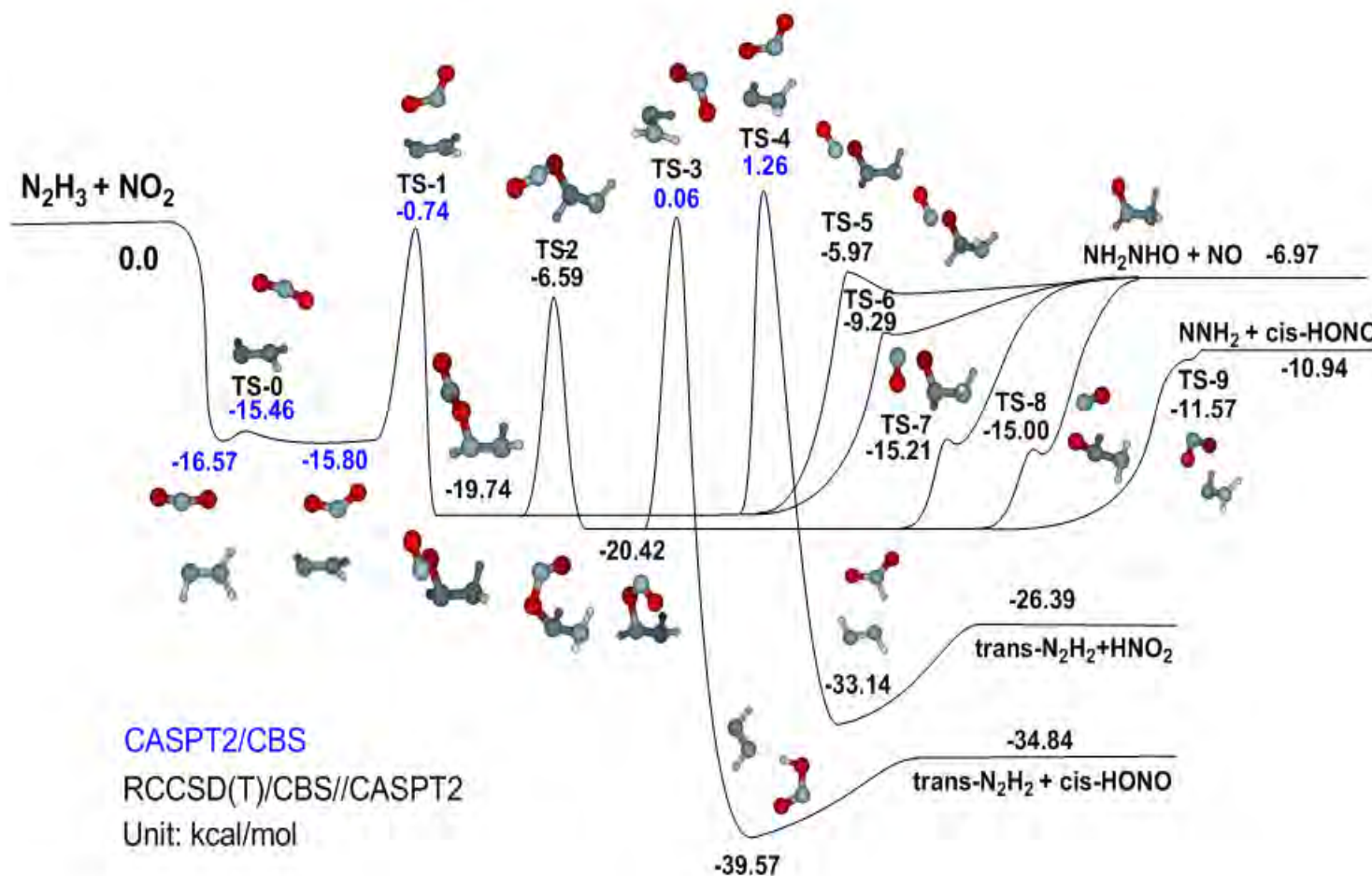
RCCSD(T)/CBS//B3LYP

Unit: kcal/mol



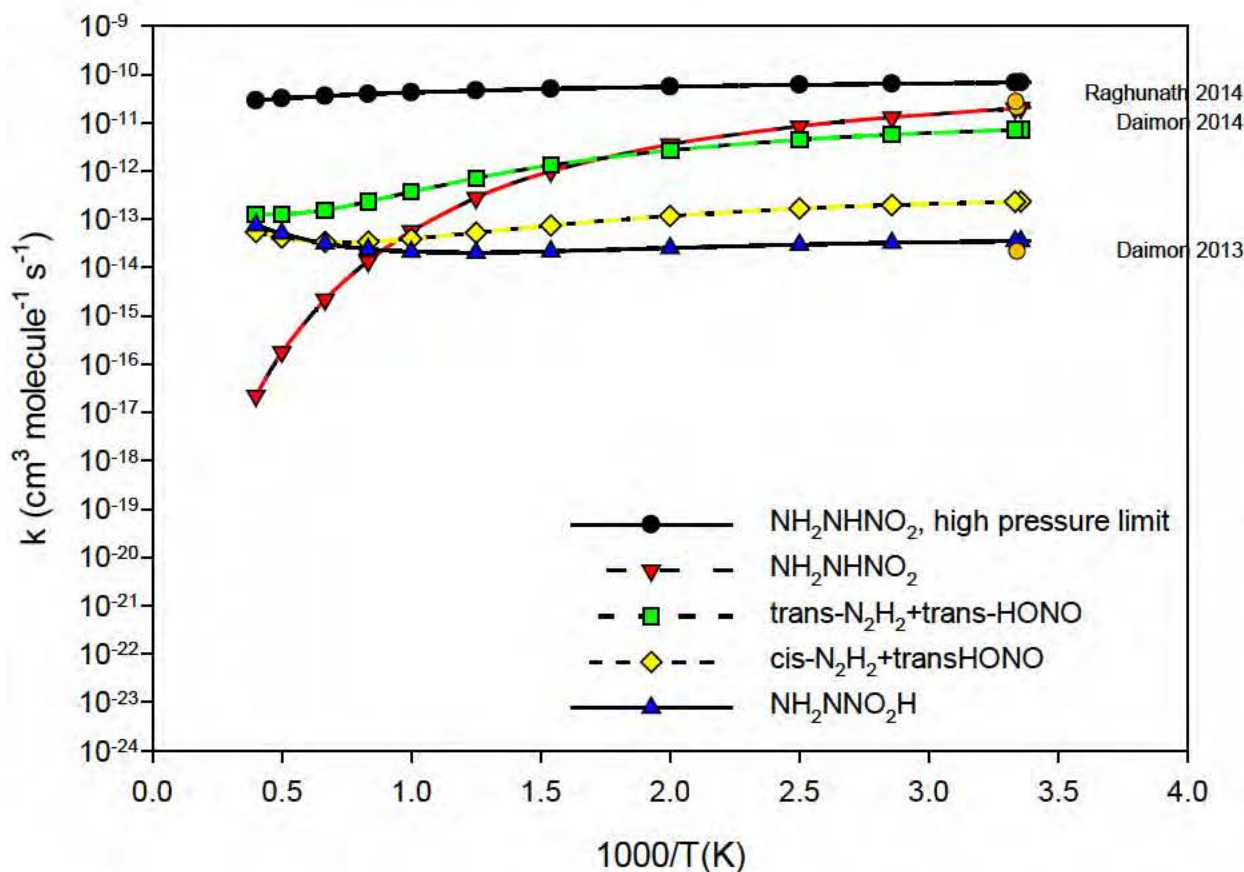


Potential Energy Surface for $\text{N}_2\text{H}_3\text{ONO}$ Adduct Formation





Branching Rate Coefficients (2 Torr N_2) & High Pressure Limit Versus T



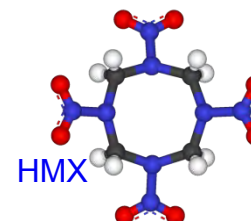


MNB & DNB Energetic Materials Perspective

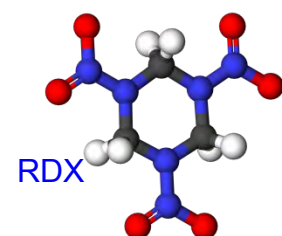


■ MNB & DNB

- Mononitrobiuret & 1,5-dinitrobiuret (less stable)
 - promising explosives



HMX



RDX

■ Recent Works

- See Geith *et al.*, *Propellants, Explosives, Pyrotechnics*, **29**, 3 (2004)
 - $\Delta H_{\text{comb}}(\text{DNB}) = (5195 \pm 300) \text{ kJ kg}^{-1}$ (bomb calorimetry and MP2/cc-pVTZ ΔH_f) cf HMX 9435 & RDX 9560 kJ kg^{-1}
 - $V_d = 8660 \text{ ms}^{-1}$, cf HMX 9100 & RDX 8750 ms^{-1}
- See Geith *et al.*, *Combust and Flame*, **139**, 358 (2004)
 - Recent synthesis (known since 1898 by Thiele) & decomposition mechanism studies
 - Initially NH_2NO_2 released, followed by residues decomposing to give HNCO
- See Liu *et al.*, *J. Phys. Chem. A* **115**, 8064 (2011) & Sun *et al.*, *J. Phys. Chem. A* **118**, 2228 (2013)
 - Quasi-classical direct dynamics trajectory simulations to understand DNB decomposition
 - Elimination of HNN(O)OH intermediate identified
- See Suntsova *et al.*, *Struct. Chem.*, **24**, 745 (2013)
 - Electronic structure of DNB was studied by two-dimensional B3LYP potential energy scans
 - Solid- and gas-phase conformers differ

■ This work

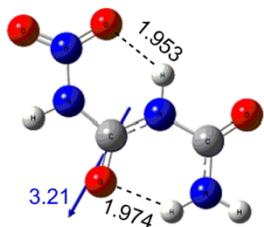
- PESs for the thermal decomposition of MNB and DNB investigated
- Temperature and pressure-dependent rate coefficients were calculated using micro-canonical transition state theory with master equation simulations



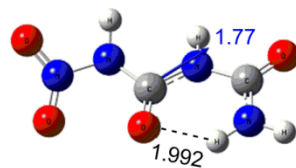
MNB & DNB Structures (M06-2X/aug-cc-pVTZ level)

■ H-bond Stabilized Conformers

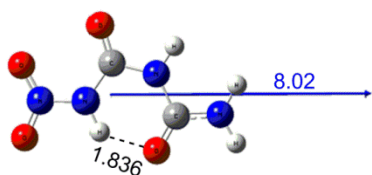
- MNB(C_s) 0
- MNB(trans) +4.82
- MNB(C_1) +6.38
- MNB(cis) +7.95 kcal/mol



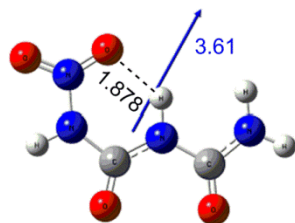
MNB (C_s)



MNB (C_1)



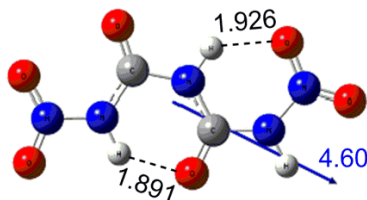
MNB (trans)



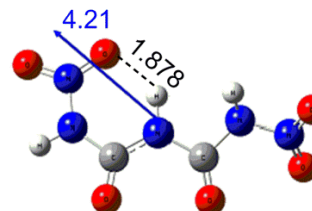
MNB (cis)

■ Double H-bond Stabilized Conformers

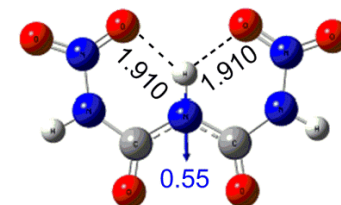
- DNB(C_s) 0
- DNB(C_{2v}) +1.22
- DNB(C_1) +7.82 kcal/mol



DNB (C_s)



DNB (C_1)



DNB (C_{2v})



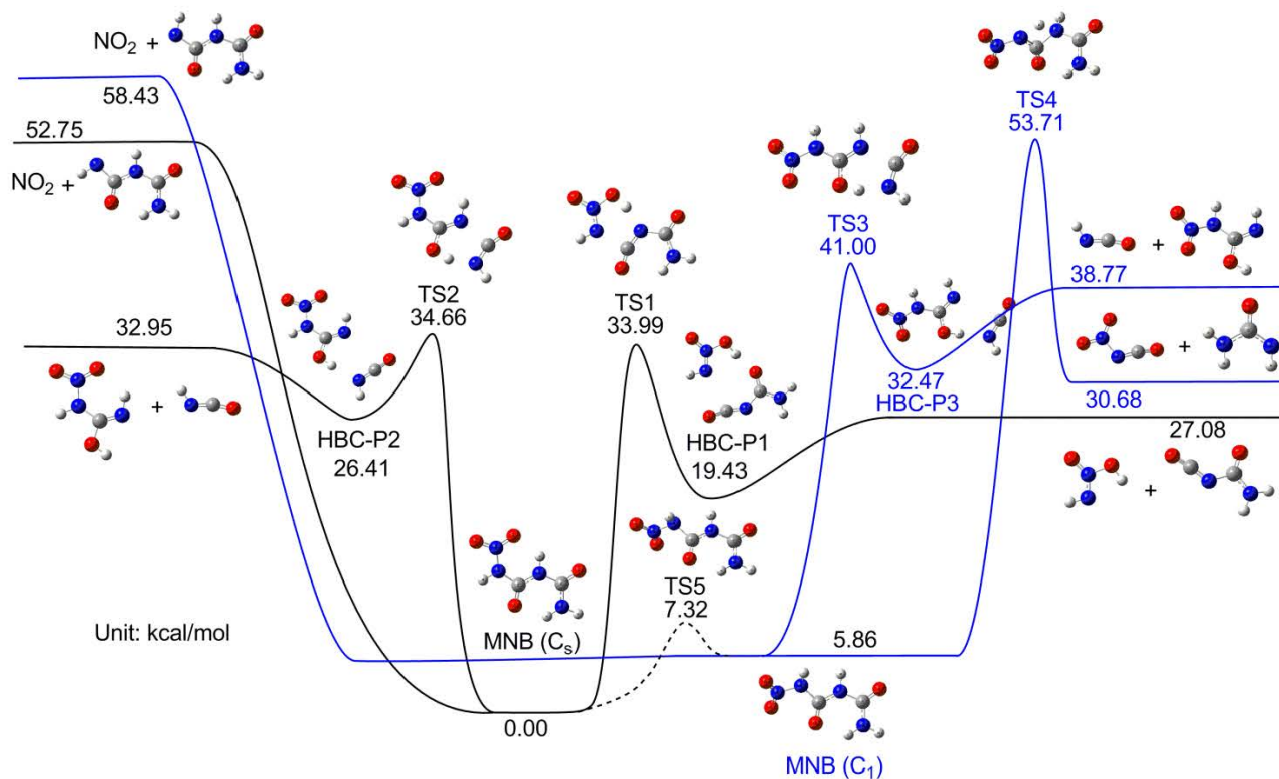
Stationary Point Energies for MNB Thermal Decomposition



Species	M06-2X /aug-cc-pVDZ	M06-2X /aug-cc-pVTZ	RCCSD(T)/cc-pV ∞ Z //M06-2X/aug-cc-pVTZ
MNB (C _s)	0.00	0.00	0.00
TS1	33.86	33.18	33.99
HBC-P1	18.50	20.51	19.43
IM1 + HNN(O)OH	29.42	26.85	27.08
TS2	34.58	33.73	34.66
HBC-P2	27.75	26.20	26.41
IM2 + HNCO	30.43	32.17	32.95
trans-biuret radical + NO ₂	51.41	51.34	52.75
MNB (C ₁)	6.41	6.38	5.86
TS3	41.05	40.35	41.00
HBC-P3	34.23	32.65	32.47
IM3 + HNCO	40.33	38.46	38.77
TS4	53.77	54.71	53.71
NH ₂ C(O)NH ₂ + NO ₂ , NCO	34.38	32.53	30.68
iso-trans-biuret radical + NO ₂	57.25	56.99	58.43
TS5	7.84	8.29	7.32

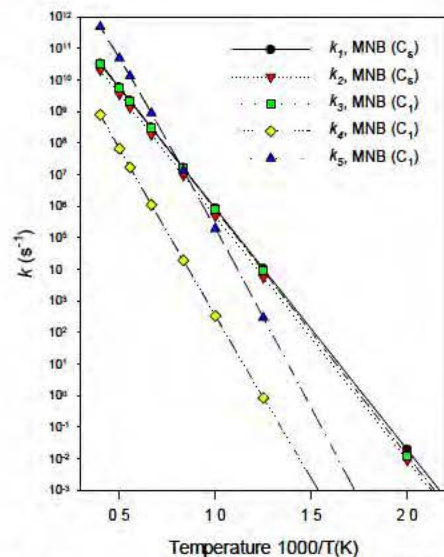
All energies include zero-point corrections and are in kcal/mol relative to the global energy minimum of MNB (C_s).

Within 1.0 kcal/mol for the barrier heights, and 1.8 kcal/mol for endothermicities compared to RCCSD(T)/cc-pV ∞ Z//M06-2X/aug-cc-pVTZ, implying that the M06-2X/aug-cc-pVTZ energies are good for larger analogous systems.





Ab initio Kinetics of MNB Thermal Decomposition

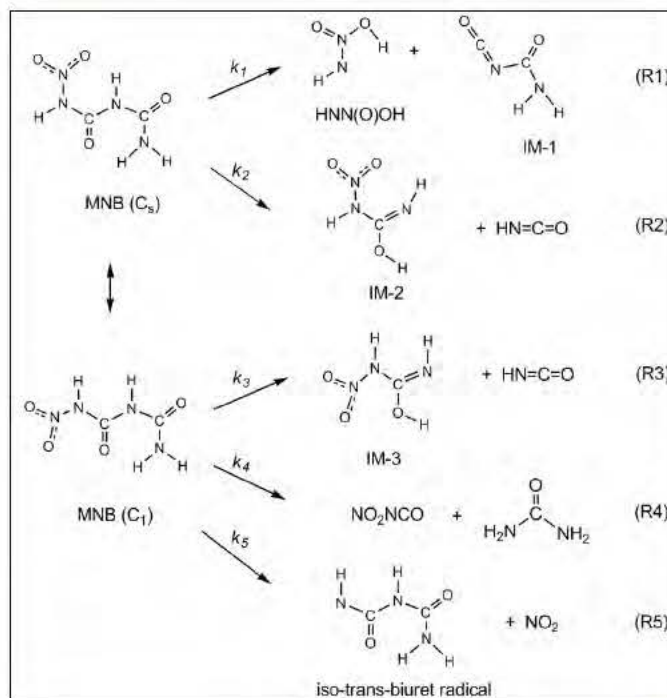


High-pressure rate limit for MNB (C_6) and MNB (C_1) primary thermal decomposition channels

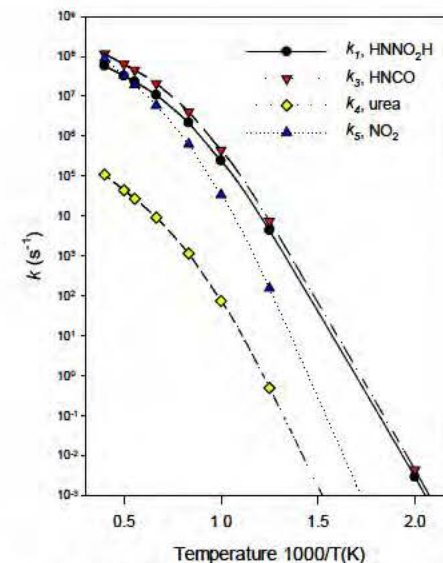
$$\begin{aligned}
 k_{1,\infty} &= 1.32 \times 10^{13} T^{0.131} \exp(-17474.7/T) \\
 k_{2,\infty} &= 1.05 \times 10^{13} T^{0.112} \exp(-17692.1/T) \\
 k_{3,\infty} &= 1.15 \times 10^{14} T^{-0.117} \exp(-18011.4/T) \\
 k_{4,\infty} &= 1.26 \times 10^4 T^{2.539} \exp(-21375.5/T) \\
 k_{5,\infty} &= 2.07 \times 10^{23} T^{-2.002} \exp(-27714.8/T)
 \end{aligned}$$

Below 1200 K, HNCO & HNN(O)OH eliminations dominate, consistent with experimental work of Gieth *et al.* 2004

Above 1200 K, NO_2 elimination dominates



MNB (C_6) and MNB (C_1) primary thermal decomposition channels



Rate coefficients at pressure of 1 atm for MNB (C_6) and MNB (C_1) primary thermal decomposition channels

Pressure dependence of unimolecular decomposition evaluated using $\Delta E_{\text{down}} = 200 \times (T/300)^{0.85} \text{ cm}^{-1}$ energy transfer probability model

Strong pressure dependences observed

HNCO & HNN(O)OH eliminations are competitive & dominate below 2500 K

NO_2 elimination becomes competitive only above 2500 K

R2 & R3 (HNCO) & R1 (HNN(O)OH) are primary (product) channels at ignition temperatures



Stationary Point Energies for DNB Thermal Decomposition



Species	M06-2X/aug-cc-pVDZ	M06-2X/aug-cc-pVTZ
DNB (C_s)	0.00	0.00
TS6	34.17	33.77
HBC-P6	21.58	20.30
HNN(O)OH + NO ₂ NHC(O)NCO	28.68	26.79
TS7	31.72	31.21
HBC-P7	30.70	29.98
IM2 + NO ₂ NCO	34.79	36.91
C ₁ -MNB radical + NO ₂	50.20	49.79
trans-MNB radical + NO ₂	50.89	51.09
DNB (C_{2v})	1.16	1.22
TS8	28.64	28.61
HBC-P8	22.35	21.70
HNN(O)OH + iso-NO ₂ NHC(O)NCO	29.08	27.26
cis-MNB radical + NO ₂	52.54	52.84
DNB (C_1)	7.45	7.82
TS9	9.42	10.32
TS10	10.79	11.20

All energies include zero-point corrections and are in kcal/mol relative to the global energy minimum of DNB (C_s).

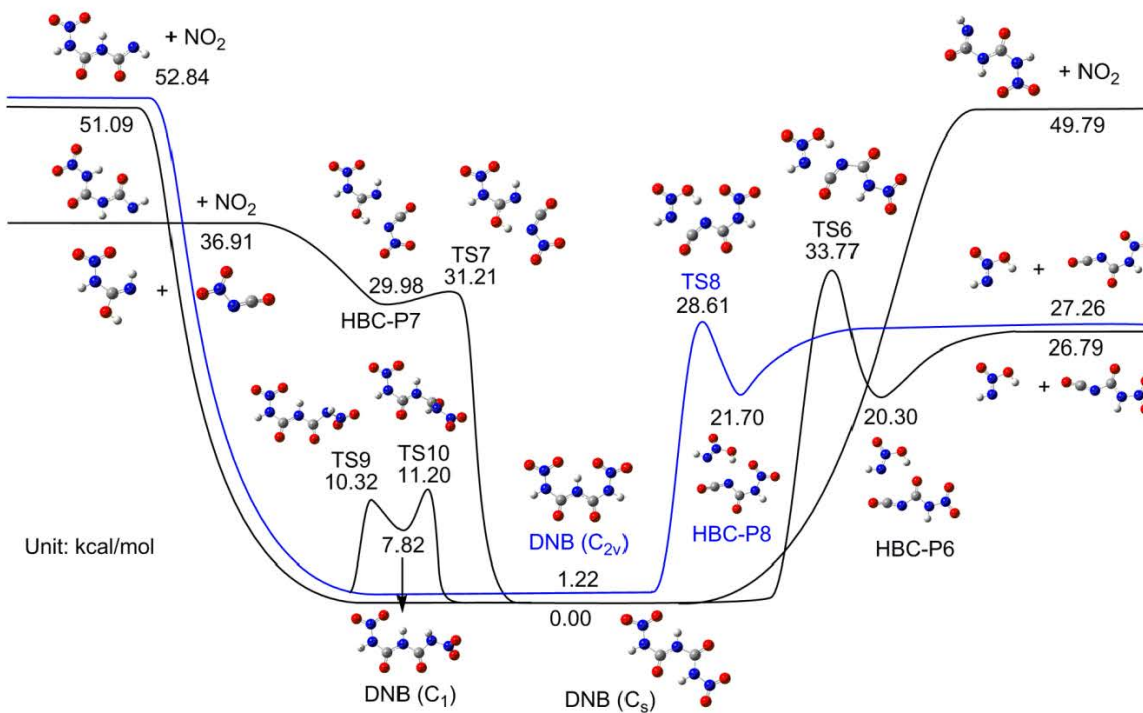
Predicted energy barrier heights from these two levels of calculation show excellent agreement, but discrepancy reaches to 2.1 kcal/mol for reaction endothermicities. Consequently, the M06-2X/aug-cc-pVTZ energies were used for carrying out the kinetics analysis for DNB decomposition.



Potential Energy Surface for DNB Decomposition

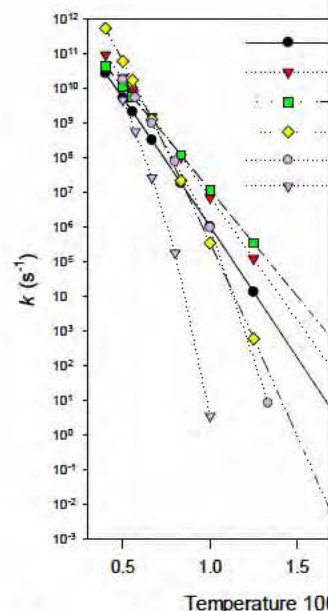


M06-2X/aug-cc-pVTZ



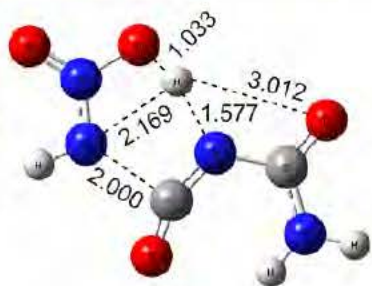


Ab initio Kinetics of DNB Thermal Decomposition

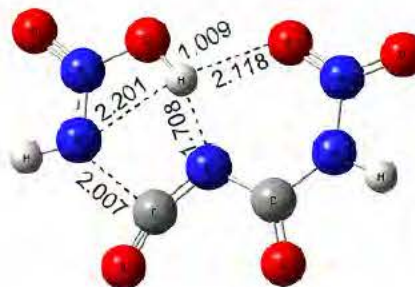


High-pressure rate limit for DNB (primary thermal decomposition)

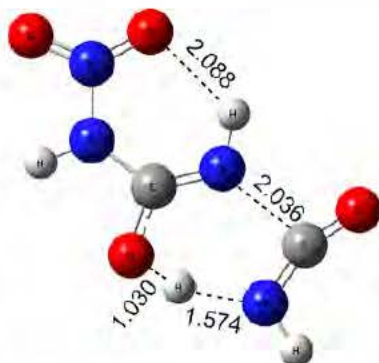
$$\begin{aligned}
 k_{6,\infty} &= 3.22 \times 10^{14} T^{-0.289} \exp(-27200.5/T) \\
 k_{7,\infty} &= 8.49 \times 10^{16} T^{-0.882} \exp(-27200.5/T) \\
 k_{8,\infty} &= 9.72 \times 10^{13} T^{-0.248} \exp(-27200.5/T) \\
 k_{9,\infty} &= 9.96 \times 10^{23} T^{-2.205} \exp(-27200.5/T)
 \end{aligned}$$



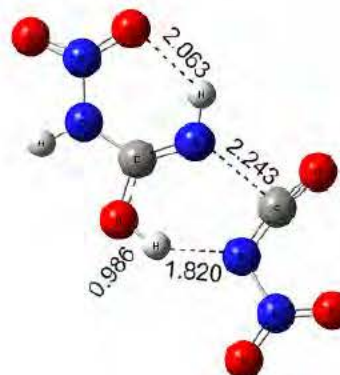
MNB (TS1)



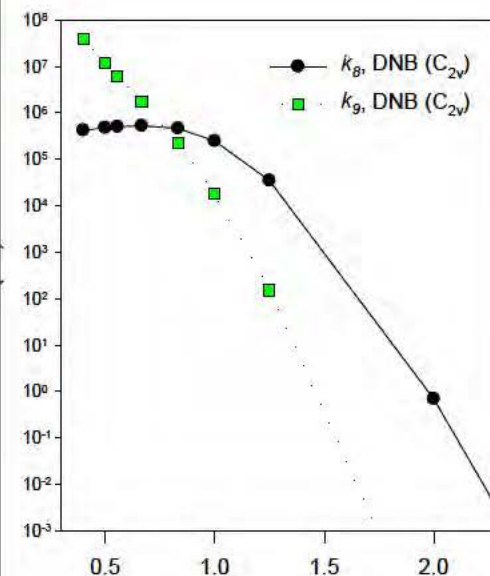
DNB (TS8)



MNB (TS2)



DNB (TS7)



Rate coefficients at pressure of 1 atm for DNB (C_{2v}) primary thermal decomposition channels

ng pressure dependences observed

w 1200 K, HNN(O)OH elimination dominates

Below 1500 K, HNN(O)OH elimination dominates from DNB (C_{2v})

Above 1500 K, NO_2 elimination dominates from DNB (C_{2v})

Similar trend seen in Liu *et al.*, 2011, and good agreement above 1500 K

k_8 for HNN(O)OH elimination from DNB is much larger than k_1 for HNN(O)OH from MNB below 800 K

Consistent with TS1 (and TS3) energy higher than TS8 (Also, TS2 higher than TS7)

TS8 is stabilized by additional intramolecular H-bonding (Also, TS7 is a late transition state)

DNB is less stable than MNB

Present quantitative interpretations are consistent with experimental work of Gieth *et al.* 2004



Conclusions & Acknowledgements



- $\text{N}_2\text{H}_3 + \text{NO}_2$ addition reaction is fast
 - $\text{trans-N}_2\text{H}_2 + \text{trans-HONO}$ main products
- PES surface characterized
 - Calculated reaction rate coefficients in agreement with experiments
- MNB & DNB stabilized via 6-member-ring moieties involving intramolecular H-bonding
 - Solid state conformers have smallest dipole moment
- Energy barriers and endothermicities at the M06-2X/aug-cc-pVTZ level of theory show remarkable agreement with the values obtained from RCCSD(T)/cc-pV ∞ Z//M06-2X/aug-cc-pVTZ computations
 - Former level of theory should be applicable to larger analogous systems
- MNB decomposition initiated by the elimination of HNCO and HNN(O)OH, the latter is also released in DNB (C_{2v}) decomposition
- Energy barrier for HNN(O)OH elimination in DNB is 6.60 kcal/mol lower than that in MNB due to an extra hydrogen bond in the transition state for the former
 - DNB less stable than MNB (as previously shown by experiments)



THE NATIONAL ACADEMIES
Advisers to the Nation on Science, Engineering, and Medicine

